CARBON 49 (2011) 193–197

available at www.sciencedirect.com

ScienceDirect

journal homepage: www.elsevier.com/locate/carbon

A theoretical evaluation of load transfer in multi-walled carbon nanotubes

Y.L. Chen [a], B. Liu [a,*], K.C. Hwang [a], Y. Huang [b]

[a] AML, Department of Engineering Mechanics, Tsinghua University, Beijing 100084, China
[b] Department of Civil and Environmental Engineering and Department of Mechanical Engineering, Northwestern University, Evanston, IL 60208, USA

ARTICLE INFO

Article history:
Received 1 July 2010
Accepted 2 September 2010
Available online 7 September 2010

ABSTRACT

Load transfer in the multi-walled carbon nanotubes (MWCNTs) is studied using a shear-lag model that accounts for the atomistic features. The analysis takes into account both the lattice registry effect and the elasticity of the CNTs. It is shown that the strength utilization ratio cannot be further improved either by increasing the CNT length beyond five times of a characteristic length, or by a change in the layer spacing, and the diameter and the chirality of the CNTs. Therefore, MWCNTs are not a good reinforcement in composites from the aspect of interwall load transfer.

1. Introduction

Carbon nanotubes (CNTs) have high strength and modulus, large aspect ratio, and low density, and are ideal candidates for reinforcements in polymer-matrix composite materials [1–4]. For multi-walled carbon nanotubes (MWCNTs), interwall load transfer is important to the effective reinforcement of CNTs. Gojny et al. [5] studied the oxidized MWCNT/epoxy composites, and found that the outermost wall remained in the matrix while the inner walls were pulled out. This suggests that the van der Waals interactions between CNT walls cannot transfer all the loads carried by the outermost wall to inner walls such that the strength of the inner walls is not reached and therefore not fully utilized in the composite material.

There are prior studies on the load transfer between CNT walls. By neglecting the effect of lattice registry, Lu et al. [6] obtained the constant load F_γ transferred between the two walls of a double-walled carbon nanotube (DWCNT) from the Lennard–Jones potential. According to this theory the inner CNT is definitely pulled out no matter of its length. Qian et al. [7] accounted for the effect of lattice registry in their study on load transfer between single-wall CNTs in a CNT rope, but neglected the elasticity of CNTs. They identified two parts of load transfer between CNTs: a constant load due to new surface formed in sliding between CNT walls, and a load resulting from lattice registry that is proportional to the overlap length between CNTs. If such an analysis were extended to the MWCNT, it would predict a long-enough inner CNT to be pulled to fracture.

By noting the opposite predictions from previous theories, this paper aims at studying the interactions between the CNT walls in order to know the strength utilization ratio of the inner CNTs, and both the elasticity and lattice registry of CNTs are taken into account. Without losing generality, only DWCNTs are studied. As schematically illustrated in Fig. 1a, the inner CNT is equivalently subject to a pulling force after the outermost wall breaks. If the resistance force between the matrix and the outer wall can be transferred to the inner wall efficiently, the strength of the inner walls is then fully utilized to improve the strength and ductility of the composite. A model for a DWCNT shown in Fig. 1b is established to study the load transfer between CNT walls.

* *Corresponding author:* Fax: +86 10 62781824.
E-mail address: liubin@tsinghua.edu.cn (B. Liu).
0008-6223/$ - see front matter
doi:10.1016/j.carbon.2010.09.003

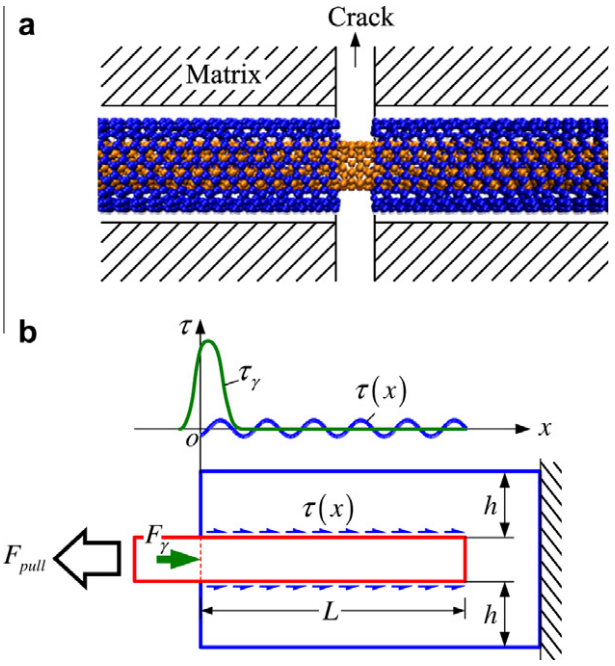

Fig. 1 – Scheme of (a) a double-walled carbon nanotube with a fractured outer wall in a composite material and (b) model for analysis with two types of shear stress on the inner wall.

2. Model

We first investigate the effect of lattice registry. The shear stress between walls is a lattice-depended periodic function related to the relative displacement $\Delta u(x) = u_{in}(x) - u_{out}(x)$, where $u_{in}(x)$ and $u_{out}(x)$ are the axial displacements of inner and outer tubes, respectively. With the atomic-scale finite element method (AFEM) [19,20], the interwall shear stress is studied by simulating the relative sliding between the inner and outer walls. In order to extract the pure effect of lattice registry, only the relative sliding and rotation are allowed, and the elastic deformation of tubes is restricted. The shear stress varies with the relative displacement periodically, as shown in Fig. 2 for (5,5)@(10,10) DWCNT. Based on this atomic simulation, the shear stress can be expressed as

$$\tau(x) = \tau^b \sin\left(\frac{\Delta u(x)}{l_0}\cdot 2\pi\right) \tag{1}$$

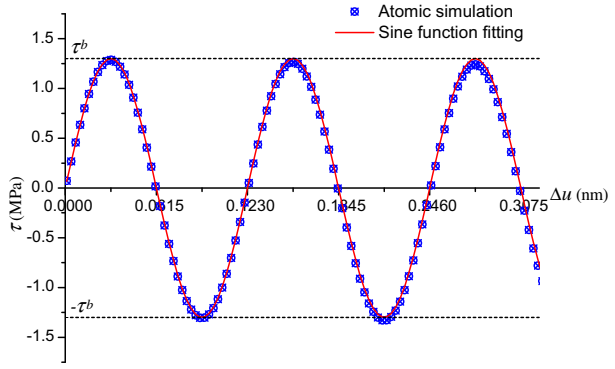

Fig. 2 – Interwall shear stress versus relative displacement for (5,5)@(10,10) CNT.

where τ^b is the maximum shear stress or the interwall shear strength, and l_0 is the periodic length determined by the carbon–carbon bond length l_{C-C} and the chirality of the CNT. For DWCNTs with armchair inner and outer walls $l_0 = \sqrt{3}l_{C-C}/2 = 0.123$ nm, and for those with zigzag inner and outer walls $l_0 = 1.5L_{C-C} = 0.213$ nm. The interwall shear strength and periodic length for the DWCNTs with different chiralities are shown in Table 1, which indicates that the DWCNTs with inner and outer walls being both armchair and both zigzag have stronger registry effect than the others.

As shown in Fig. 1b, the periodic shear stress $\tau(x)$ distributes throughout the whole overlap area. While for the atoms close to the two ends of the overlap segment ($x = 0$ and $x = L$ in Fig. 1b), the shear stress caused by the newly formed surface should also be considered. The van der Waals interactions between a pair of carbon atoms I and J of distance r can be characterized by the Lennard–Jones potential $V(r) = 4\varepsilon_{IJ}(\sigma_{IJ}^{12}/r^{12} - \sigma_{IJ}^{6}/r^{6})$, where $\varepsilon_{IJ} = 2.39$ meV and $\sigma_{IJ} = 0.3415$ nm for carbon atoms [8]. This new surface related shear stress is denoted as τ_γ in Fig. 1b, and can be integrated as a total force applied on the ends as [6]

$$F_\gamma = 2\pi^2 d\rho_C^2\varepsilon_{IJ}\sigma_{IJ}^2\left[\frac{\sigma_{IJ}^4}{h^4} - \frac{2\sigma_{IJ}^{10}}{5h^{10}}\right] \tag{2}$$

where d is the average diameter of inner and outer walls, h is the layer spacing (i.e., the radial distance between the inner and outer walls) and $\rho_C = 4/(3\sqrt{3}l_{C-C}^2)$ is the number of carbon atoms per unit area on the CNT.

3. Shear-lag-model-based stress analysis for the DWCNTs

Due to the constraint from the matrix material, we assume that the outer tube is rigid, and the inner wall is linear elastic, with the stiffness $E_{in}A_{in}$. The equilibrium equation for the inner wall can then be expressed based on the shear-lag theory [9–13] as

$$\begin{aligned} A_{in}\sigma_{in}(x) &= F_{pull} - F_\gamma - \int_0^x \pi d\tau(x)dx = E_{in}A_{in}\varepsilon_{in}(x) \\ &= E_{in}A_{in}\frac{du_{in}(x)}{dx} \end{aligned} \tag{3}$$

where F_{pull} is the pulling force. From Eqs. (1) and (3), the governing equation for $u_{in}(x)$ is obtained as

$$\frac{1}{b^2}\sin\left(\frac{u_{in}(x)}{l_0}\cdot 2\pi\right) = \frac{d^2\left(\frac{u_{in}(x)}{l_0}\cdot 2\pi\right)}{dx^2} \tag{4}$$

where $b = \sqrt{\frac{E_{in}A_{in}l_0}{2\pi^2 d\tau^b}}$ is a characteristic length depending on the properties of the CNT. The following two boundary conditions can be obtained from the equilibrium of the inner wall at $x = 0$ and $x = L$

$$\left.\frac{du_{in}(x)}{dx}\right|_{x=0} = \frac{F_{pull} - F_\gamma}{E_{in}A_{in}} \tag{5}$$

$$F_{pull} - F_\gamma = \pi d\tau^b \int_0^L \sin\left(\frac{u_{in}(x)}{l_0}\cdot 2\pi\right)dx \tag{6}$$

Usually, it is difficult to derive the analytical solution for Eqs. (4)–(6). For the following special cases the analytical solution can be obtained and degenerated into previous theories.

Table 1 – The interwall shear strength and periodic length for different DWCNTs.

Chirality	(5,5)@(10,10)	(9,0)@(18,0)	(9,0)@(10,10)	(6,3)@(18,0)	(6,4)@(12,8)
τ^b (MPa)	1.30	19.3	0.436	0.397	0.627
l_0 (nm)	0.123	0.213	0.123	0.213	0.0491

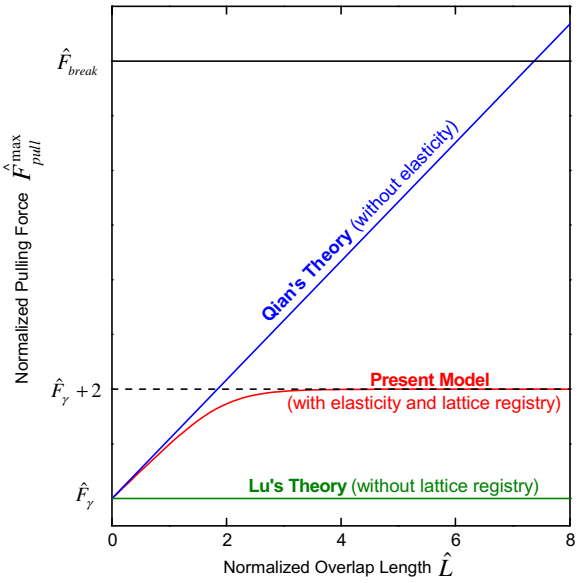

Fig. 3 – Normalized pulling force as a function of normalized overlap length of DWCNTs.

Case 1: Neglecting the lattice registry, i.e., $\tau^b = 0$, Eq. (6) becomes

$$F_{\text{pull}} = F_\gamma \tag{7}$$

It is exactly Lu et al.'s theory [6], which predicts a constant pulling force irrelevant to the CNT length, as shown in Fig. 3.

Case 2: Neglecting the elastic deformation of CNT, i.e., $E_{\text{in}}A_{\text{in}} \to \infty$, it is concluded from Eqs. (4)–(6) that the displacement u_{in} is independent of x, and the pulling force becomes

$$F_{\text{pull}} = F_\gamma + \pi d\tau^b \sin\left(\frac{u_{\text{in}}}{l_0}\cdot 2\pi\right)L \tag{8}$$

Eq. (8) indicates that the load transferred between CNT walls is composed of two parts: a constant load due to new surface formed in sliding between CNT walls and a load proportional to the overlap length, as shown in Fig. 3. This is exactly the same as Qian et al.'s theory [7].

For general situation, numerical solution can be obtained, and the normalized parameters $\hat{x} = x/b$, $\hat{L} = L/b$, $\hat{F}_{\text{pull}} = F_{\text{pull}}/(b\pi d\tau^b)$, $\hat{F}_\gamma = F_\gamma/(b\pi d\tau^b)$, and $\hat{u}_{\text{in}}(\hat{x}) = 2\pi u_{\text{in}}(x)/l_0$ are used. The normalized pulling force $\hat{F}_{\text{pull}}$ depends on not only the normalized overlap length $\hat{L}$, but also the normalized pulling-out displacement $\hat{u}_{\text{in}}(0)$. The maximum normalized pulling force is defined as $\hat{F}_{\text{pull}}^{\max}(\hat{L}) = \max_{\hat{u}_{\text{in}}(0)}\left[\hat{F}_{\text{pull}}(\hat{u}_{\text{in}}(0),\hat{L})\right]$.

Numerical analysis shows that the normalized maximum pulling force $\hat{F}_{\text{pull}}^{\max}$ increases with the increase of the normalized overlap length $\hat{L}$, and finally it goes asymptotically to a constant. It can be proved analytically that the constant is

$$\hat{F}_{\text{pull}}^{\max}(\hat{L}\to\infty) = \hat{F}_\gamma + 2 \tag{9}$$

The inner tube only breaks if the maximum axial normal force reaches the CNT strength, and the corresponding critical pulling force is F_{break}. Thus the pullout/break critical condition is

$$F_{\text{pull}}^{\max}/F_{\text{break}} = 1 \text{ or } \hat{F}_{\text{pull}}^{\max}/\hat{F}_{\text{break}} = 1 \tag{10}$$

where $\hat{F}_{\text{break}} = F_{\text{break}}/(b\pi d\tau^b)$. If $F_{\text{pull}}^{\max}/F_{\text{break}} < 1$ the inner tube can be pulled out without breaking. We define the strength utilization ratio of the inner tube as $F_{\text{pull}}^{\max}/F_{\text{break}}$ to measure the load transfer between the walls. If this ratio becomes 1, the strength of inner tube can be used completely. The upper limit of the strength utilization ratio can be estimated as

$$\frac{F_{\text{pull}}^{\max}}{F_{\text{break}}} < \frac{F_{\text{pull}}^{\max}(\hat{L}\to\infty)}{F_{\text{break}}} = \frac{F_\gamma + \sqrt{2E_{\text{in}}A_{\text{in}}l_0 d\tau^b}}{F_{\text{break}}} \tag{11}$$

So with a weak interwall shear strength, i.e., $\tau^b < \frac{(F_{\text{break}}-F_\gamma)^2}{2E_{\text{in}}A_{\text{in}}l_0 d}$, the inner tube cannot break no matter how long it is, as shown in Fig. 3.

4. Factors affecting strength utilization ratio of the inner tube

The properties of the CNT in above equations and figures ($E_{\text{in}}A_{\text{in}}$, τ^b, F_{break}) can be easily obtained from previous works [14–20]. Among them the atomic-scale finite element method (AFEM) [19,20] is adopted to obtain these parameters.

Taking (5,5)@(10,10) DWCNT for an example, the atomic simulation on axial tension provides the stiffness $E_{\text{in}}A_{\text{in}} = 582$ nN and the critical pulling force $F_{\text{break}} = 75.35$ nN; the atomic simulation on relative sliding provides the interwall shear strength $\tau^b \cdot \pi d = 0.004174$ nN/nm. So the maximum strength utilization ratio of the inner tube, which is defined as $F_{\text{pull}}^{\max}(L\to\infty)/F_{\text{break}}$, can be obtained as

$$F_{\text{pull}}^{\max}(L\to\infty)/F_{\text{break}} = (\hat{F}_\gamma + 2)/\hat{F}_{\text{break}} = 1.62\% \tag{12}$$

where $\hat{F}_\gamma = 3.61$ is obtained from Eq. (2), and $\hat{F}_{\text{break}} = F_{\text{break}}/(b\pi d\tau^b) = 345.6$.

Using this method, various influence factors affecting the maximum strength utilization ratio of the inner tube (i.e., $F_{\text{pull}}^{\max}/F_{\text{break}}$) are discussed below, including the overlap length, the interwall spacing, the diameter and the chirality of the CNT.

4.1. *Effect of overlap length*

Qian et al.'s theory [7] believes that the longer overlap length leads to larger maximum pulling force $\hat{F}_{\text{pull}}^{\max}$, so increasing the overlap length can always improve the inner tube strength utilization ratio $F_{\text{pull}}^{\max}/F_{\text{break}}$ effectively. However, by taking

Table 2 – The inner CNT strength utilization ratio for various DWCNTs.

Chirality	(5,5)@(10,10)	(5,5)@(9,9)	(5,5)@(8,8)	(10,10)@(15,15)	(9,0)@(16,0)	(9,0)@(14,0)
Layer spacing h (nm)	0.3375	0.2925	0.2682	0.3394	0.2946	0.2670
Maximum inner CNT strength utilization ratio $F_{\text{pull}}^{\max}(L\to\infty)/F_{\text{break}}$	1.62%	2.71%	3.56%	1.34%	15.03%	26.94%

the elasticity into account, the present model predicts that $\hat{F}_{\text{pull}}^{\max}$ increases with the increase of $\hat{L}$ but quickly approaches its upper limit $\hat{F}_{\text{pull}}^{\max}(\hat{L}\to\infty)$, as shown in Fig. 3. When the normalized overlap length $\hat{L}=5$, the maximum pulling force $\hat{F}_{\text{pull}}^{\max}(\hat{L}=5)$ has already been very close to its upper limit $\hat{F}_{\text{pull}}^{\max}(\hat{L}\to\infty)$. For the (5,5)@(10,10) CNT when $L=240$ nm and for the (9,0)@(18,0) when $L=95$ nm, the maximum pulling force $\hat{F}_{\text{pull}}^{\max}$ only have 0.03% difference from $\hat{F}_{\text{pull}}^{\max}(\hat{L}\to\infty)$. So far the length of the CNTs can reach the order of centimeter, and therefore the efforts to make longer CNTs cannot increase the inner tube strength utilization ratio effectively.

4.2. *Effect of layer spacing*

Interwall shear strength τ^b is an explicit parameter to present the load transfer between the inner and outer walls. Can the inner tube strength utilization ratio be improved by increasing the interwall shear strength? Xu et al. [21] proved interwall shear strength increased with the decrease of the layer spacing. The reduced graphite layer spacing can be formed by electron irradiation of graphitic carbon materials [22,23]. Is it possible to make the layer spacing small enough such that the inner tube strength is fully utilized and the failure mode transits from pullout to break? A series of DWCNTs with (5,5) inner tube (i.e., (5,5)@(n,n) CNTs) are studied, and the maximum inner tube strength utilization ratios $F_{\text{pull}}^{\max}(L\to\infty)/F_{\text{break}}$ for different outer tube (different reduced layer spacing) are shown in Table 2. It shows that the maximum inner tube strength utilization ratio increases with the decrease of layer spacing. However, this increase is very limited and the failure mode is always inner tube pullout. Before the reduced layer spacing causes the topology change (break and reform of the covalent bond) for (5,5)@(7,7) CNT, the maximum inner tube strength utilization ratio can be increased to 3.56%.

4.3. *Effect of diameter*

Our analysis indicates that both $F_{\text{pull}}^{\max}$ and F_{break} are proportional to the diameter d for the same type of CNTs (e.g., two armchair CNTs). So the inner tube strength utilization ratio should be roughly independent of the diameter. Table 2 shows that with the same layer spacing, the maximum inner tube strength utilization ratio of smaller diameter ((5,5)@(10,10) CNT) is close to that of larger diameter ((10,10)@(15,15) CNT), which implies that the diameter only have very slight effect on the inner tube strength utilization ratio.

4.4. *Effect of chirality*

To investigate the chirality effect, the results of both zigzag and armchair DWCNTs are studied and shown in Table 2. For the same diameter and layer spacing (e.g. (9,0)@(16,0) versus (5,5)@(9,9), and (9,0)@(14,0) versus (5,5)@(8,8)), the inner tube strength utilization ratio of zigzag DWCNTs is much higher than that of the armchair ones. This means the zigzag DWCNTs are more capable to transfer the load than the armchair ones. Therefore, the chirality has great effect on the inner tube strength utilization ratio, because the chirality dominates the effect of lattice registry, which is the origin of the interwall shear stress. The inner and outer walls with the same chirality have strong lattice registry effect. However, the chiralities for the inner and outer walls are usually random and thus the inner tube strength utilization ratio is much lower than the cases in Table 2. For example, (7,2)@(11,8) CNT has similar radius and layer spacing to (5,5)@(10,10) CNT and (9,0)@(18,0) CNT, but the inner tube strength utilization ratio is only 1.07%, while (5,5)@(10,10) CNT is 1.62% and (9,0)@(18,0) CNT is 5.18%.

With the lattice registry effect taken into account, the results from this paper are obviously different from Lu et al.'s work [6], especially for the DWCNTs with same chirality and reduced layer spacing. For (9,0)@(16,0) and (9,0)@(14,0) CNTs, the relative errors $[F_{\text{pull}}^{\max}(L\to\infty)-F_{\gamma}]/F_{\text{pull}}^{\max}(L\to\infty)$ are up to 99.5% and 114%, respectively. However, for most CNTs (random chirality and normal layer spacing), the effect of lattice registry is much weaker and accordingly the relative error is much lower. Take (7,2)@(14,5) CNT as an example. The relative error is only 8.7%. So Lu et al.'s theory [16] can make a simple and reasonable prediction for the DWCNTs with weak lattice registry and normal layer spacing.

5. Conclusions

The extended shear-lag theory with periodic shear stress is developed in this paper. It is concluded that from the aspect of interwall load transfer neither DWCNTs nor MWCNTs are a good reinforcement in composites, because the strength of the inner tube cannot be fully utilized. Single-walled CNTs are more suitable to reinforce the composite materials under tension. A large diameter MWCNT may be more desirable than an equal diameter SWNT because it can better resist bending, buckling, and collapse during manufacturing. So in CNT-reinforced composites design, all the factors should be considered comprehensively to choose the correct CNTs. It should be pointed out that the theoretical analysis and the conclusions in this paper can also be extended to other interwall interactions with periodic shear stress, such as the interactions among CNTs in a CNT bundle and on the periodic CNT/matrix interface in CNT-reinforced composites.

Acknowledgments

The authors acknowledges the support from National Natural Science Foundation of China (Grant Nos. 10702034, 10732050,

90816006, and 10820101048), and National Basic Research Program of China (973 Program) Grant Nos. 2007CB936803 and 2010CB832701.

REFERENCES

[1] Qian D, Dickey EC, Andrew R, Rantell T. Load transfer and deformation mechanisms in carbon nanotube–polystyrene composites. Appl Phys Lett 2000;76(20):2868–70.
[2] Lourie O, Wagner HD. Transmission electron microscopy observations of fracture of single-wall carbon nanotubes under axial tension. Appl Phys Lett 1998;73(24):3527–9.
[3] Cooper CA, Cohen SR, Barber AH, Wagner HD. Detachment of nanotubes from a polymer matrix. Appl Phys Lett 2002;81(20):3873–5.
[4] Thostenson ET, Chou TW. Aligned multi-walled carbon nanotube-reinforced composites: processing and mechanical characterization. J Phys D Appl Phys 2002;35:77–80.
[5] Gojny FH, Nastalczyk J, Roslaniec Z, Schulte K. Surface modified multi-walled carbon nanotubes in CNT/epoxy-composites. Chem Phys Lett 2003;370:820–4.
[6] Lu WB, Wu J, Jiang LY, Huang Y. A cohesive law for multi-wall carbon nanotubes. Philos Mag 2007;87:2221–32.
[7] Qian D, Liu WK, Rodney S, Ruoff RS. Load transfer mechanism in carbon nanotube rope. Compos Sci Technol 2003;63:1561–9.
[8] Girifalco L, Hodak AM, Lee RS. Carbon nanotubes, buckyballs, ropes, and a universal graphitic potential. Phys Rev B 2000;62:13104–9.
[9] Cox HL. The elasticity and strength of paper and other fiberous materials. Br J Appl Phys 1952;3:72–9.
[10] Chon CT, Sun CT. Stress distributions along a short fibre in fibre reinforced plastics. J Mater Sci 1980;15:931–8.
[11] Hutchinson JW. Models of fiber debonding and pullout in brittle composites with friction. Mech Mater 1990;9:139–63.
[12] Budiansky B, Evans AG, Hutchinson JW. Fiber-matrix debonding effects on cracking in aligned fiber ceramic composites. Int J Solids Struct 1995;32:315–28.
[13] Chen YL, Liu B, Wu J, Huang Y, Jiang H, Hwang KC. Failure analysis and the optimal toughness design of carbon nanotube-reinforced composites. Compos Sci Technol 2010;70(9):1360–7.
[14] Zhang P, Huang Y, Geubelle PH, Klein PA, Hwang KC. The elastic modulus of single-wall carbon nanotubes: a continuum analysis incorporating interatomic potentials. Int J Solids Struct 2002;39:3893–906.
[15] Jiang H, Zhang P, Liu B, Huang Y, Geubelle PH, Gao H, et al. The effect of nanotube radius on the constitutive model for carbon nanotubes. Comput Mater Sci 2003;28:429–42.
[16] Arroyo M, Belytschko T. An atomistic-based finite deformation membrane for single layer crystalline films. J Mech Phys Solids 2002;50(9):1941–77.
[17] Belytschko T, Xiao SP, Schatz GC, Ruoff RS. Atomistic simulations of nanotube fracture. Phys Rev B 2002;65(23):235430/1–8.
[18] Chen YL, Liu B, Wu J, Huang Y, Jiang H, Hwang KC. Mechanics of hydrogen storage in carbon nanotubes. J Mech Phys Solids 2008;56:3224–41.
[19] Liu B, Huang Y, Jiang H, Qu S, Hwang KC. The atomic-scale finite element method. Comput Meth Appl Mech Eng 2004;193:1849–64.
[20] Liu B, Jiang H, Huang Y, Qu S, Yu M.-F. Atomic-scale finite element method in multiscale computation with applications to carbon nanotubes. Phys Rev B 2005;72(3):035435/1–8.
[21] Xu ZP, Wang LF, Zheng QS. Condensed multiwalled carbon nanotubes as super fibers. Small 2008;4(6):733–7.
[22] Banhart F, Ajayan PM. Carbon onions as nanoscopic pressure cells for diamond formation. Nature 1996;382:433–5.
[23] Sun L, Banhart F, Krasheninnikov AV, Rodríguez-Manzo JA, Terrones M, Ajayan PM. Carbon nanotubes as high-pressure cylinders and nanoextruders. Science 2006;312:1199–202.